A Four Degree of Freedom MEMS Microgripper with Novel Bi-Directional Thermal Actuators

Michael A. Greminger A. Serdar Sezen
Department of Mechanical Engineering
University of Minnesota
Minneapolis, MN 55455
{grem,ssezen}@me.umn.edu

Bradley J. Nelson
Institute of Robotics and Intelligent Systems
Swiss Federal Institute of Technology (ETH)
CH-8092 Zurich, Switzerland
bnelson@ethz.ch

***Abstract*— A four degree of freedom thermally actuated MEMS microgripper is presented in this paper. Each jaw of the microgripper has independent x and y degrees of freedom. These extra degrees of freedom give the gripper added dexterity for manipulating microparts. The motion of each gripper jaw is provided by a two degree of freedom compliant mechanism which is based on a five bar rigid link mechanism. This gripper also introduces a novel thermal microactuator design that is capable of bi-directional actuation giving it a greater range of motion than previous thermal actuator designs. The actuator provides a total range of motion of 12.7 μm and a maximum force of 1.9 mN. Also, since this microgripper is based on a compliant mechanism, deformable object tracking can be used to provide force as well as position feedback for the gripper. This combination of an increased number of degrees of freedom and increased sensory feedback provides a level of dexterity that has not been previously available in microassembly.**

***Index Terms*— Microgripper, microassembly, microrobotics, MEMS, compliant mechanism.**

I. Introduction

Microrobotic systems are currently used for many applications in microassembly [3] [15] and in biomanipulation [2] [13]. Microrobotic systems hold much promise. However, the capabilities of these systems are limited when compared to their macroscale counterparts. For example, microgrippers typically are limited to a single degree of freedom for both actuation and feedback. Greater end effector dexterity and sensory feedback is required to produce more advanced microrobotic systems. This paper presents technology that will help to increase capabilities of microrobotic systems by presenting a microgripper that both provides increased dexterity and the potential for increased sensory feedback when compared to previous designs.

In this paper, a four degree of freedom bulk micromachined MEMS microgripper is presented. Each jaw of the microgripper is a compliant mechanism with both an x and a y degree of freedom. A bi-directional bending thermal actuator is used for each degree of freedom. The thermal actuator is able to bend in either direction because the electric circuit is completed through the kinematic chain of the compliant mechanism. Therefore, the location of heating within the mechanism can be controlled remotely by applying electrical potential at the appropriate contacts.

Force feedback can also be provided for the microgripper design presented in this paper. Since compliant mechanisms are used to provide the motion of the gripper jaws, the deformations of these compliant mechanisms can be tracked visually to provide force feedback through the use of vision-based force measurement. Force feedback can be provided for each degree of freedom of the gripper. It has been shown that vision-based force measurement provides a robust and non-contact approach for providing force feedback in microsystems [4] [5] [14].

This paper is organized as follows. First the design of the microgripper is discussed. The design of both the compliant mechanism and the design of the thermal actuators are addressed. Next, the fabrication and instrumentation of the microgripper is presented. Finally, the characteristics and performance of the devices and their actuators are presented.

II. Design

The design goal for this microgripper is for each jaw of the gripper to have both x and y degrees of freedom. Typically, MEMS microgrippers only possess a single degree of freedom which opens and closes the gripper. The addition of these three extra degrees of freedom gives the gripper added dexterity.

A compliant mechanism is used for each jaw of the microgripper to give it the necessary degrees of freedom. The compliant mechanism design is based off of a five bar rigid link mechanism. The design of the thermal actuators used to actuate the device is also discussed in this section.

A. Mechanism Design

The design of the compliant mechanism for each jaw of the gripper is based off of a five bar mechanism design. A five bar mechanism has two degrees of freedom. The input to the mechanism is the rotation angle of each of the links attached to ground as shown in Figure 1. The position of the entire mechanism is completely determined by the position of these two input links.

The design objectives for the compliant mechanism are to decouple each of the degrees of freedom and to amplify the motion of the actuator inputs. The mechanism design that is used for each jaw of the gripper is shown in Figure 2(a).

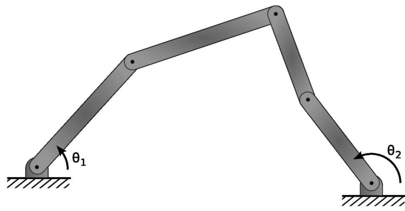

Fig. 1. Five bar rigid link mechanism.

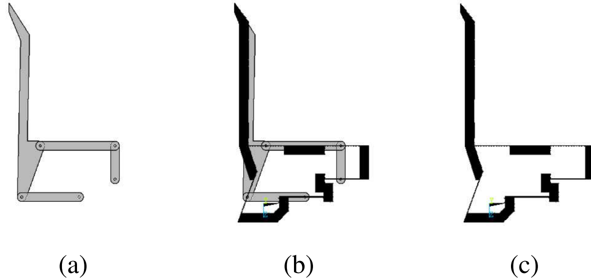

Fig. 2. A compliant mechanism (c) based on a rigid link mechanism (a).

The paths followed by the a gripper jaw for each degree of freedom are shown in Figures 3(a) and (b). It can be seen that the degrees of freedom are nearly completely decoupled.

A compliant mechanism is created from the rigid mechanism by using a compliant member to approximate each pivot joint in the rigid link design. Each compliant member is a flexible beam with the center point of the beam lying at the location of the pivot it replaces. The length of each of the compliant members affects how closely the motion of the compliant mechanism approximates that of the rigid link mechanism. The shorter the compliant members, the closer the motion of the compliant mechanism matches that of the rigid link mechanism. The drawback of short compliant links is that they experience greater internal stresses for the same level of gripper motion as compared to longer compliant members. Finite element simulations of the compliant mechanism were used to evaluate the kinematic performance of the compliant mechanism as well as to insure that the compliant members will not fail under normal operating conditions. Simulation results for each degree of freedom are shown in Figures 3(c) and (d).

B. Actuator Design

Both electrostatic actuators and thermal actuators were considered as the source of actuation for each degree of freedom of the microgripper. Thermal actuation was chosen for two reasons. The first is that electrostatic actuators could not provide the forces necessary to actuate the compliant mechanism without requiring excessive device area or extremely high actuation voltages. Second, electrostatic actuators are most effective at providing linear actuation whereas the gripper's compliant mechanism requires a rotational input. Bending thermal actuators naturally provide a rotational motion.

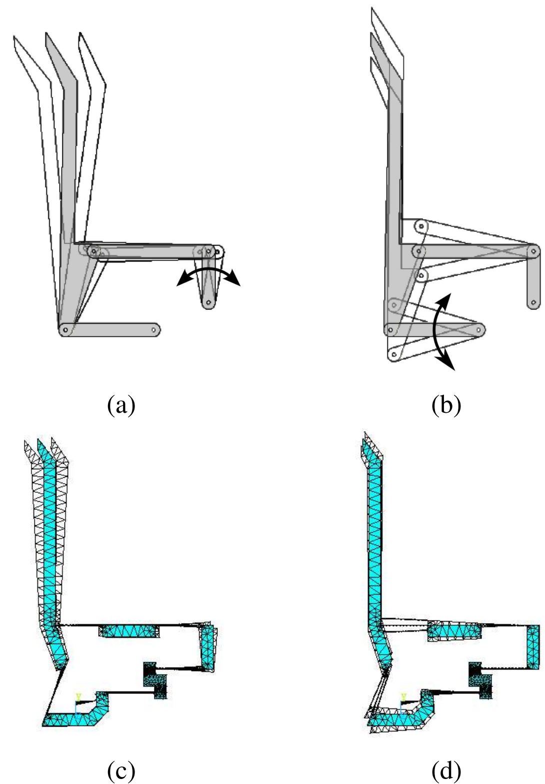

Fig. 3. Degrees of freedom for the rigid link mechanism (a)(b) and the associated compliant mechanism (c)(d).

All thermal actuators deflect as the result of an applied thermal stress where heating is generally provided by Joule heating. Thermal stresses arise in three situations: when there is a nonhomogeneous temperature distribution in a structure; when there is a nonhomogeneous coefficient of thermal expansion and the temperature changes; and when a structure is overly constrained and the temperature is changed thus causing buckling. Thermal actuators using each of these mechanisms are currently implemented in MEMS devices. The commonly used MEMS thermal actuators are shown in Figure 4. Figure 4(a) shows a thermal actuator that relies on nonuniform temperature distribution [6] [7], Figure 4(b) shows a thermal actuator based on the buckling principle [9] [12], and Figure 4(c) shows a thermal actuator that relies on a nonhomogeneous coefficient of thermal expansion [1] [10]. The limitation of each of these designs is that they can only be actuated in a single direction.

The thermal actuator design that is proposed here is shown in Figure 5. As can be seen from the figure, depending on which contacts electrical potential is applied to, the actuator can be actuated in either direction. This is possible because the compliant mechanism itself is used to close the electrical path, thus providing a return path for the current used to heat the hot arm of the actuator. In order to control this type of an actuator with a computer, an interface which converts the signal level voltages from the computer to currents has been designed. This circuit is discussed in Section III-B. The

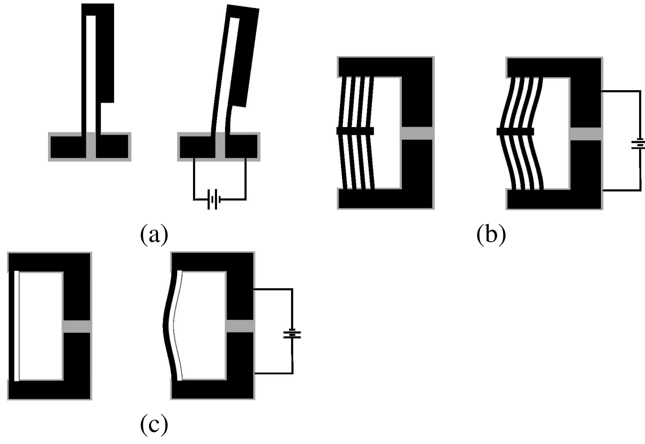

Fig. 4. Common thermal actuator designs: (a) bending thermal actuator, (b) buckling beam thermal actuator, and (c) bimorph thermal actuator.

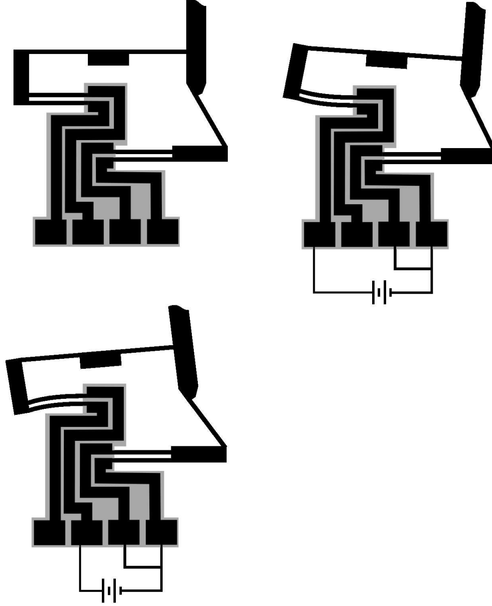

Fig. 5. The thermal actuator design introduced in this paper.

limitation of this type of actuator is that it can only be used in a situation where the actuator is connected to a closed kinematic chain. However, when a closed kinematic chain is being used, this design is superior to the previous actuator technologies because it can be actuated in two directions.

The displacement of this actuator design can be estimated by modeling the actuator as two parallel beams separated by an air gap. The beams are clamped on both ends as shown in Figure 6(a). The properties of each of the beams are identical with the only difference being the temperature. This temperature difference induces a stress which results in a deflection of the beam. The actuator is in a state of pure bending when the beams are at different temperatures. The effective bending moment associated with this state of pure bending is [8]:

$$M = \frac{eEA\alpha}{2}\left(T_2 - T_1\right) \tag{1}$$

where A is the cross sectional area of each beam, T_1 and T_2 are the temperatures of beams 1 and 2 respectively, e is the distance between the centers of the beams, and α is the coefficient of thermal expansion for both of the beams. The moment M is the moment that would have to be applied to the end of the undeflected actuator to cause it to deflect the same magnitude as when the temperatures of beam 1 and 2 are T_1 and T_2 respectively. The radius of curvature ρ of the actuator is related to the bending moment by the following:

$$\frac{1}{\rho} = \frac{M}{EI} = \frac{eA\alpha}{2I}\left(T_2 - T_1\right) \tag{2}$$

where I is the moment of inertia of both beams together and is defined as:

$$I = 2\left(\frac{bh^3}{12} + \frac{Ae^2}{4}\right) \tag{3}$$

where h is the height of each beam and b is the depth of each beam. From the curvature of the beam, the total deflection of the actuator can be calculated using the following equation [16]:

$$\delta = \frac{l^2}{2\rho} = \frac{eA\alpha l^2}{4I}\left(T_2 - T_1\right) \tag{4}$$

where l is the length of the actuator. It can be seen from the above equation that the deflection of the actuator is proportional to the temperature difference between the two beams. The maximum actuation force can also be calculated in terms of the temperature difference between the beams. The maximum force that the actuator can supply is equivalent to the force F required to keep the end of the actuator from moving when a moment M of magnitude (1) is applied to the end of the beam (see Figure 6(c)). The equation for F is [16]:

$$F = \frac{3EI}{2l\rho} = \frac{3eEA\alpha}{4l}\left(T_2 - T_1\right) \tag{5}$$

This is the force that the actuator can generate at zero deflection which is referred to as the blocking force. The force that the actuator can generate decreases as the actuator travels through its range of motion.

III. Fabrication and Instrumentation

The microgripper is bulk micromachined from 100 μm thick <100> silicon with less than 0.01 Ohm-cm resistivity. This 100 μm silicon layer makes up the device layer of a silicon-on-oxide (SOI) wafer which has a 2 μm silicon-dioxide box layer and a 250 μm thick silicon handle layer. The oxide layer serves both as an etch stop layer during fabrication and as an electrical insulator for the final device. Deep reactive ion etching (DRIE) is used to create the microgripper's features.

After the microgripper is fabricated it needs to be interfaced with a circuit to provide current to actuate the thermal actuators. An interface circuit was designed so that voltages

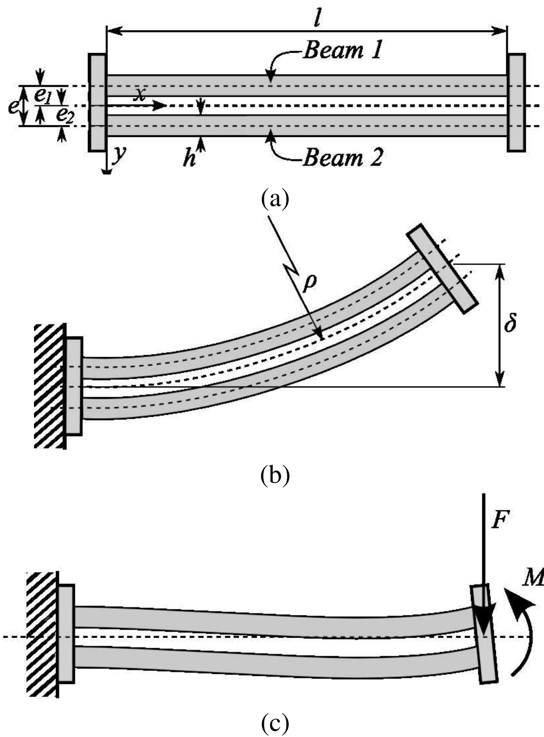

Fig. 6. Model used to calculate the displacement of the actuator and the maximum force of the actuator.

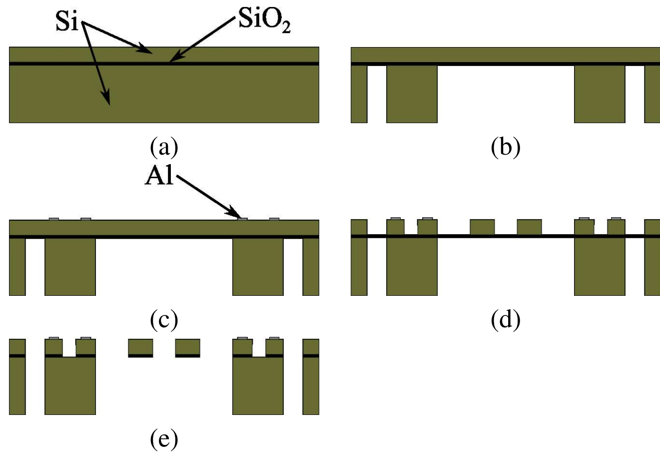

Fig. 7. Fabrication sequence used to fabricate the microgripper.

from a digital to analog converter can be used to control the displacement of the actuators.

A. Fabrication Process

The fabrication sequence is outlined in Figure 7. The SOI wafer that forms the starting point is shown in Figure 7(a). The first step is to etch the handle layer of the wafer using DRIE (see Figure 7(b)). This step forms the frame and the support structure for the final device. Figure 7(c) shows the next step which is to pattern the aluminum contacts that are used to electrically connect the device to its control circuit. The next step is to etch the device layer (see Figure 7(d)).

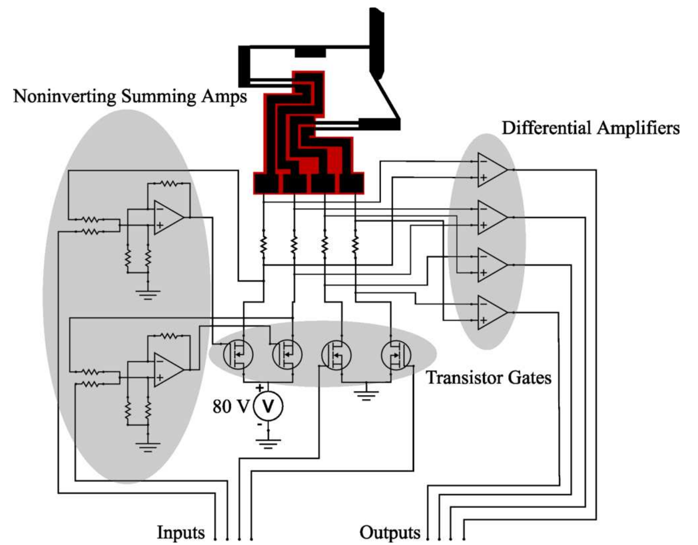

Fig. 8. Interface circuit used to control the gripper with signal level voltage inputs.

The device layer that remains after this etching step forms the geometry of the gripper jaws, the compliant mechanisms, and the thermal actuators. Finally, the devices are released from the wafer by etching away the exposed oxide (see Figure 7(e)). The oxide is etched using a plasma etcher.

B. Instrumentation

An interface circuit was implemented so that voltages from a digital to analog converter can be used to control the motion of the gripper. The direction of actuation and which actuator are actuated depend on the path the electrical current takes through the device. Transistors are used as gates to control this path. The state of the transistors determines which of the two actuators is activated and the direction of actuation. A simplified version of the interface circuit is is shown in Figure 8 for one jaw of the microgripper. The input to the circuit is the gate voltage to each of the transistors. The input voltage is boosted using noninverting summing amplifiers for the transistors on the high voltage side of the circuit because the gate voltage required for these transistors is above signal levels. The supply voltage to the circuit is 80 volts. The voltage required to actuate the device to full scale deflection is 40 volts. The circuit runs at above 40 volts to account for voltage drops at the gate transistors.

Shunt resisters are placed in series with each electrical contact of the device. The voltage drop across each of these resisters is measured by a differential amplifier to provide a voltage proportional to the current entering the device. These current measurements are the output of the interface circuit and are used for two purposes. The first is to provide feedback for the user of the device. The second is to provide feedback for a current limiting circuit that is not shown. The current limiting circuit limits the maximum amount of current that can be run through the device. The current limiting circuit protects the device from being damaged by overheating. This

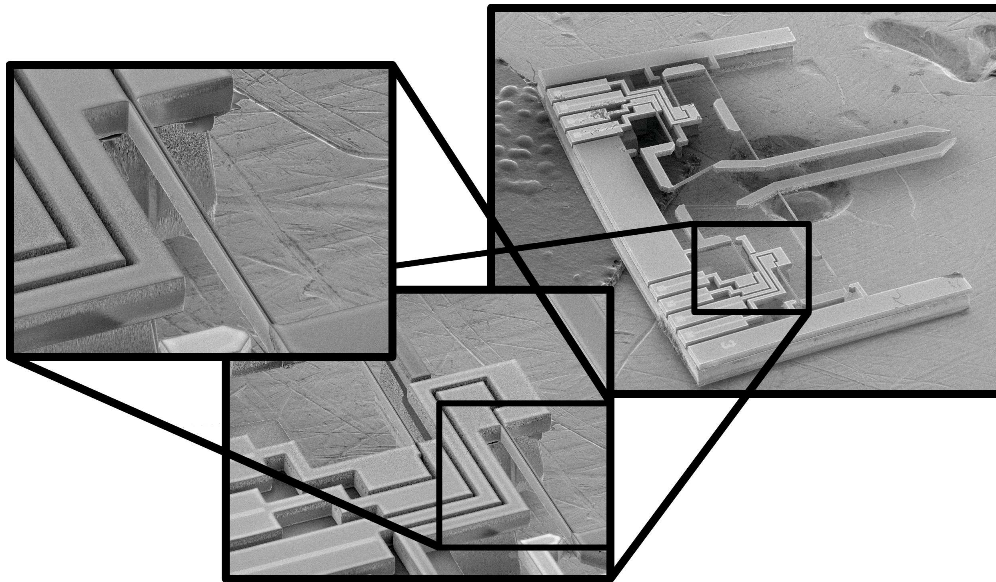

Fig. 9. SEM image of the fabricated microgripper. This device is 6mm by 6mm in size. The insets show a closeup of one of the thermal actuators.

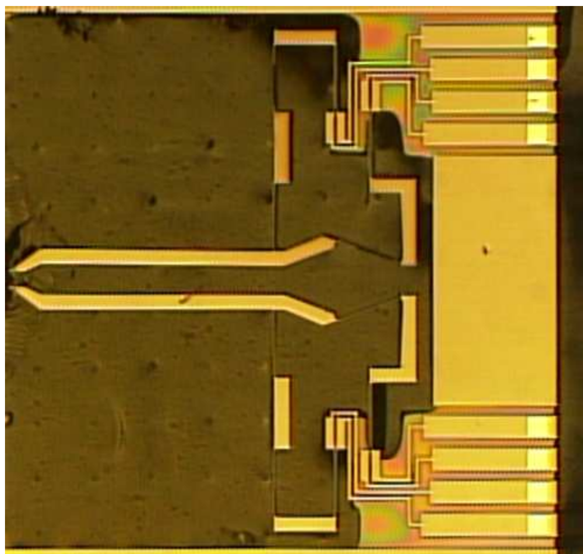

Fig. 10. Image of fabricated microgripper. This device is 3 mm by 3 mm.

limiting is important because in order to achieve the most performance out of the thermal actuators it is desirable to operate them as hot as possible without overheating them. Any control input can be sent to the device and the current limiting circuit insures that the device will not be overheated.

IV. Results

Figure 9 shows an SEM image of a fabricated device. A microscope image of another device is shown in Figure 10. This device has an overall size of 3 mm by 3 mm and is used for the results presented in this paper. Figure 11 shows the range of motion of the microgripper jaws for each of their degrees of freedom. The opening and closing range of motion for each gripper jaw is 38.4 μm, and the orthogonal range of motion for each gripper jaw is 11.6 μm.

The motion of a thermal actuator is shown in Figure 12. The total range of motion for this actuator is 12.7 μm. The actuator shown is 400 μm long, 100 μm deep, has beams that are 4 μm thick, and has a 10 μm gap between the beams. Using (4), the amplitude of deflection shown corresponds to a temperature difference of 578 $^{\circ}$C between the hot and cold beams. The maximum force that this actuator can produce is 1.9 mN, which is calculated using (5).

For the results given here, the achievable actuator deflection was limited because the compliant members of the compliant mechanism overheated before the actuator could reach its maximum temperature. This is due to increased Joule heating of the compliant members as compared to the thermal actuator beams. This occurs even though the actuator beams and the compliant members were designed to have the same thickness. The compliant members are thinner in the final device because of the ununiform etching rate of DRIE. The problem of compliant member heating can be solved in future designs by patterning a metal conductor onto the compliant members. This fix would allow the actuators to reach their maximum temperature without concern that the compliant members will overheat.

V. Conclusions and Discussion

A new gripper design has been presented that offers greater dexterity then is currently available. It also introduces a novel thermal actuator design that takes advantage of the closed kinematic chain design of the compliant mechanism to allow actuation in two directions. It was also discussed how vision-based force measurement can be used to provide position and

force feedback for the microgripper which will aid in the micromanipulation task.

Improving the dexterity and the sensing capabilities of micromanipulators will greatly enhance the cababilities of micromanipulation and biomanipulation systems. These capabilities will allow the algorithms and techniques used in macromanipulation to be applied to micromanipulation.

ACKNOWLEDGMENTS

This research was supported in part by the National Science Foundation through Grant Numbers IIS-9996061 and IIS-0208564. Michael Greminger is supported by the Computational Science Graduate Fellowship (CSGF) from the Department of Energy.

REFERENCES

[1] Benecke, W., Riethmuller, W., "Applications of silicon-microactuators based on bimorph structure," *Micro Electro Mechanical Systems, Proceedings, 'An Investigation of Micro Structures, Sensors, Actuators, Machines and Robots'*, pp. 116 - 120, Feb. 20-22, 1989.

[2] Chronis, N., Lee, L.P., "Polymer MEMS-based microgripper for single cell manipulation, " *17th IEEE International Conference on Micro Electro Mechanical Systems (MEMS2004),* pp:17 - 20, 2004, 2004.

[3] Dechev, N., Cleghorn, W.L., Mills, J.K., "Microassembly of 3-D microstructures using a compliant, passive microgripper," *Journal of Microelectromechanical Systems,* vol. 13, no. 2, pp. 176 - 189, April 2004.

[4] Greminger, M.A., Nelson, B.J., "Vision-Based Force Measurement," *IEEE Transactions on Pattern Analysis and Machine Intelligence,* Vol. 26, No. 3, pp. 290-298, March 2004.

[5] Greminger, M.A., Nelson, B.J., "Deformable object tracking using the boundary element method," *IEEE Computer Society Conference on Computer Vision and Pattern Recognition (CVPR2003),*Vol. 1, pp. 289 -294, June 2003.

[6] Guckel, H., Klein, J., Christenson, T., Skrobis, K., Laudon, M., Lovell, E.G., "Thermo-Magnetic Metal Flecture Actuators," *Proceedings of the 5th IEEE Solid-State Sensor and Actuator Workshop,*, Hilton Head Island, SC, USA, June 22-25, 1992.

[7] Huang, Q.A., Lee, N.K.S., "Analysis and design of polysilicon thermal flexure actuator," *Journal of Micromechanics and Microengineering,* vol. 9, no. 1, pp. 64-70, March 1999.

[8] Noda, N., Hetnarski, R.B., Tanigawa, Y., *Thermal Stress, 2nd ed.,*Taylor and Francis, London, 2003.

[9] Que, L., Park, J.S., Gianchandani, Y.B., "Bent-beam electro-thermal actuators for high force applications," *Twelfth IEEE International Conference on Micro Electro Mechanical Systems (MEMS99),*, pp. 31 - 36, Jan. 17-21, 1999.

[10] Riethmüller, W., Benecke, W., "Thermally Excited Silicon Microactuators," *IEEE Transactions on Electron Devices,*vol. 35, no. 6, pp. 758 - 763, June 1988.

[11] Rohsenow, W.M., Hartnett, J.P., Ganic, E.N., *Handbook of Heat Transfer Fundamentals, 2nd ed.,* McGraw-Hill, New York, 1985.

[12] Sinclair, M.J., "A high force low area mems thermal actuator," *The Seventh Intersociety Conference on Thermal and Thermomechanical Phenomena in Electronic Systems,*vol. 1 ,pp. 127-132, May 23-26, 2000.

[13] Sun, Y., Greminger, M.A., Nelson, B.J., "Investigating Protein Structure Change in the Zona Pellucida with a Microrobotic System," *International Journal of Robotics Research,* 2004.

[14] Wang, X., Ananthasuresh, G. K., Ostrowski, J. P., "Vision-based sensing of forces in elastic objects," *Sensors and Actuators A-Physical,* Vol. 94, No. 3, pp. 142-156, November 2001.

[15] Yesin, K.B., Nelson, B.J., "A CAD-Model Based Tracking System for Visually Guided Microassembly," *Robotica,* 2004.

[16] Young, W.C., Budynas, R., *Roark's Formulas for Stress and Strain, 7th ed.,*McGraw-Hill, New York, 2001.

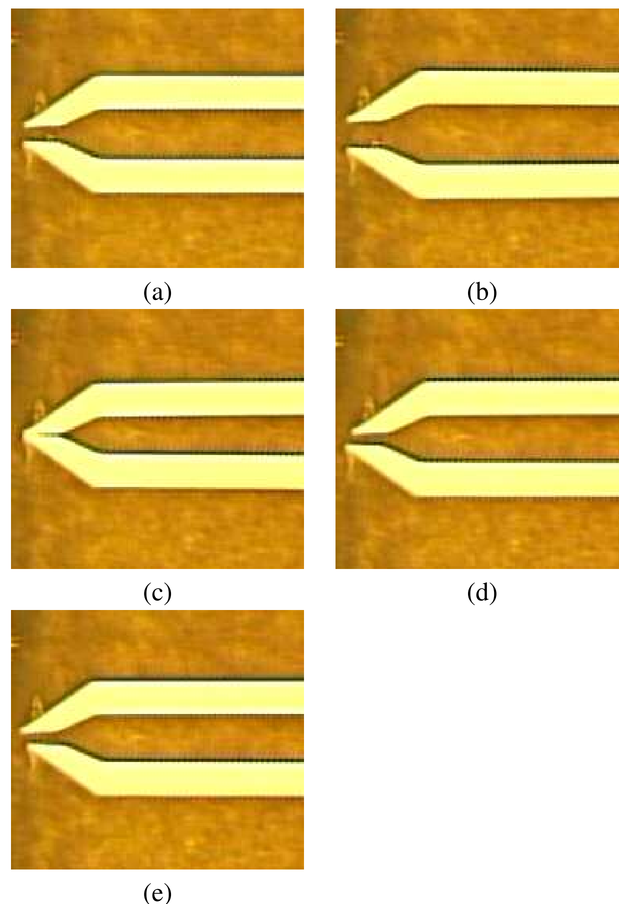

Fig. 11. Range of motion for the microgripper jaws. The undeformed microgripper is shown in (a).

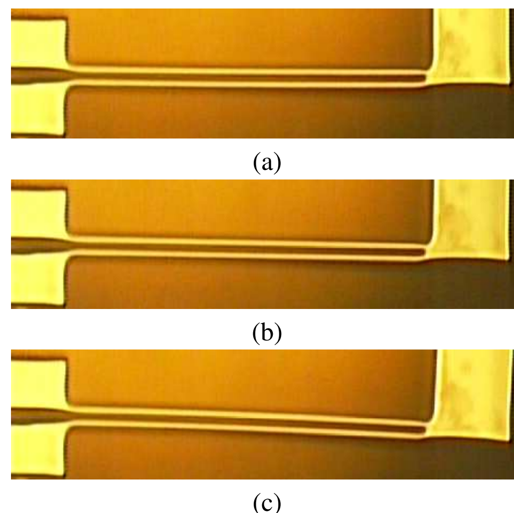

Fig. 12. Thermal actuator motion: (a) actuator deflecting upwards, (b) actuator undeflected, and (c) actuator deflecting downwards. A total displacement of 12.7 μm is shown.